

Acoustic Characteristics of 3-D Membrane-embedded-type Metamaterials

Y. Li¹, † X. M. Wang¹, *Y. L. Mei²

¹School of Mechanical Engineering, Dalian University of Technology, China.

²School of Automotive Engineering, Dalian University of Technology, China.

*Presenting author: meiyulin@dlut.edu.cn

†Corresponding author: meiyulin@dlut.edu.cn

Abstract

Researches on manipulating acoustic waves by anisotropic materials, especially, acoustic metamaterials, have received much attention. In this paper, an attempt is made to develop a new kind of 3-D acoustic metamaterial, which is constructed by embedding high-modulus membranes into soft isotropic materials. To begin with, two unit cell models of the acoustic metamaterials are established, which have an embedded single-layer membrane or embedded double-layer membranes. Then dispersion characteristics of the unit cells in the low frequency range are simulated by the finite element method; meanwhile, considering different angles of incidence of elastic waves, we use the transient response full integration method and the asymptotic homogenization method to calculate average velocities of elastic waves propagating in the unit cells. Subsequently, influences of structure parameters of the unit cells on the wave velocities are investigated. In the end, we establish a full wave simulation model of the three-dimensional membrane-embedded-type acoustic metamaterial and illustrate the propagation characteristics of acoustic waves in the metamaterial.

Keywords: Acoustic metamaterials; Membrane-embedded; Dispersion characteristics; Effective material parameters; Wave propagation

Introduction

Recently, researchers pay more attention to studies of manipulating acoustic waves by acoustic metamaterials, including acoustic cloaks, perfect focusing acoustic lenses and acoustic omnidirectional absorbers [1]-[3]. In general, acoustic metamaterials are constructed by periodically embedding local oscillators into base materials to produce local resonance, or embedding materials with high-contrast modulus into acoustic materials to cause multiple scattering of acoustic waves, or directly tailoring solid materials based on homogenization theory. In 2008, Mei, Yang et al. investigate a membrane-type acoustic metamaterial by means of simulation and experiment, where a small mass block is placed at the center of a membrane as a source of local resonance to realize acoustic absorption within the low frequency range [4]. Subsequently, researches on membrane-type acoustic metamaterials mainly highlight mechanical properties of the elastic membranes, such as ultra-thin size and ultra-light weight. And the acoustic characteristics of the metamaterials as well as the locally resonant frequencies and vibration modes can be designed, to some extent, by adjusting sizes of membranes, pre-stress applied in membranes and shapes of mass block [5]-[7]. However, most of the work focuses on acoustic insulation and absorption performance, and there has been very little study of controlling wave propagation paths in the membrane-type acoustic metamaterials. And related studies refer to active acoustic metamaterials, for example, Popa et al. design a class of tunable active acoustic metamaterials by using piezoelectric membranes

in 2013 [8].

Metamaterials with strong acoustic anisotropy can make acoustic propagation paths bend drastically, like curving and distorting, which is significant for practical acoustics problems with limited design spaces. In the paper, a kind of 3-D membrane-embedded-type acoustic metamaterial is constructed by embedding high-modulus membranes into low-modulus materials, where the in-plane stiffness of the embedded membrane is greatly different from the out-of-plane stiffness. In principle, the strong acoustic anisotropy of the metamaterials can be obtained by virtue of compositing isotropic materials with high-contrast modulus, and the directivity of wave propagation and dispersion characteristics of metamaterials can be controlled by tailoring the membranes or adjusting tensions or pre-deformations of the membranes. We mainly address acoustic characteristics of the membrane-embedded-type metamaterials, unit cells of which consist of soft rubber and a single-layer membrane or double-layer membranes. Firstly, dispersion characteristics of the unit cells are investigated in the low frequency range by the finite element method. Secondly, considering different incidence angles of acoustic waves, average velocities of wave propagation are calculated by both the transient response full integration method and the asymptotic homogenization method. Subsequently, influences of structure parameters of the unit cells on the acoustic wave velocities are studied. Finally, numerical examples are given to illustrate the wave propagation from homogeneous rubber materials to anisotropic composite materials consisting of rubber and embedded multi-layer membranes.

Unit cell models and analysis theory

According to the elastic dynamic theory, if an elastic wave propagates in the linear elastic and anisotropic inhomogeneous media, without regard to damping and external excitation, the wave equation can be expressed as

$$\nabla \cdot [\mathbf{C}(\mathbf{r}) : \nabla \mathbf{u}] = \rho(\mathbf{r}) \frac{\partial^2 \mathbf{u}}{\partial t^2} \quad (1)$$

Where $\mathbf{r} = (x, y, z)$ are position vectors, $\mathbf{C}(\mathbf{r})$ and $\rho(\mathbf{r})$ are elasticity tensors and mass-density tensors, respectively; $\mathbf{u} = (u_x, u_y, u_z)$ are displacement vectors; $\nabla = (\partial / \partial x, \partial / \partial y, \partial / \partial z)$ stands for the differential operator; the colon “:” means double dot product; t is the time variable.

For a periodic structure consisting of unit cells, according to Bloch’s theorem of periodic differential equations, we have

$$\mathbf{u}(\mathbf{r}) = e^{i(\mathbf{k} \cdot \mathbf{r})} \mathbf{u}_{\mathbf{k}}(\mathbf{r}) \quad (2)$$

Where $i = \sqrt{-1}$, $\mathbf{k} = (k_x, k_y, k_z)$ are wave numbers, $\mathbf{u}_{\mathbf{k}}(\mathbf{r})$ is a periodic function with the same period as one of the periodic structure. Considering periodicity of the structure, in order to reduce the redundant calculation, we just analyze dispersion characteristics of a unit cell. During solving the wave equation by the finite element method, the unit cell is discretized and its eigen circular frequencies ω associated with the eigenmodes \mathbf{U} satisfy

$$(\mathbf{K} - \omega^2 \mathbf{M}) \mathbf{U} = \mathbf{0} \quad (3)$$

Where, $\mathbf{K} = \int \mathbf{B}^T \mathbf{C}(\mathbf{r}) \mathbf{B} dV_e$ is the stiffness matrix, $\mathbf{M} = \int \rho(\mathbf{r}) \mathbf{N}^T \mathbf{N} dV_e$ is the mass matrix, V_e is the space occupied by the unit cell, $\mathbf{U} = [\mathbf{U}_1 \cdots \mathbf{U}_i \cdots \mathbf{U}_n]^T$ is the displacement matrix,

$\mathbf{U}_i = [u_i \ v_i \ w_i]^T$ ($i=1,2,\dots,n$) is the node displacement. If we use “a” to represent the lattice constant, the boundary condition for the unit cell can be written as

$$\mathbf{U}(\mathbf{r} + \mathbf{a}) = e^{i(\mathbf{k}\cdot\mathbf{a})}\mathbf{U}(\mathbf{r}) \quad (4)$$

The unit cell is a symmetric structure as shown in Fig.1 or Fig.2, where a single-layer membrane or double-layer membranes are embedded into a soft isotropic material. The cross-section of the membrane is square, and its thickness is h_m ; in Fig.1, h_z is the embedded depth of the single-layer membrane; in Fig.2, ΔH is the distance between the embedded double-layer membranes. It is assumed that the membrane is made of iron, and the material parameters are as follows: the modulus of elasticity $E_m = 2.1 \times 10^{11} Pa$, Poisson's ratio $\nu_m = 0.3$ and the density $\rho_m = 7860 kg/m^3$. Meanwhile, we choose rubber as the soft isotropic material, and the material parameters are the modulus of elasticity $E_r = 7.8 \times 10^6 Pa$, Poisson's ratio $\nu_r = 0.47$ and the density $\rho_r = 980 kg/m^3$.

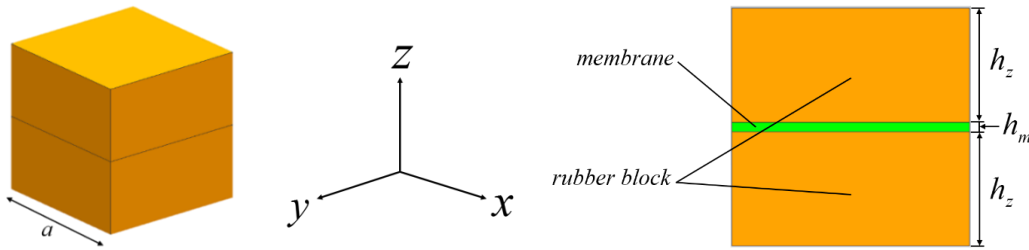


Figure 1. Unit cell with an embedded single-layer membrane

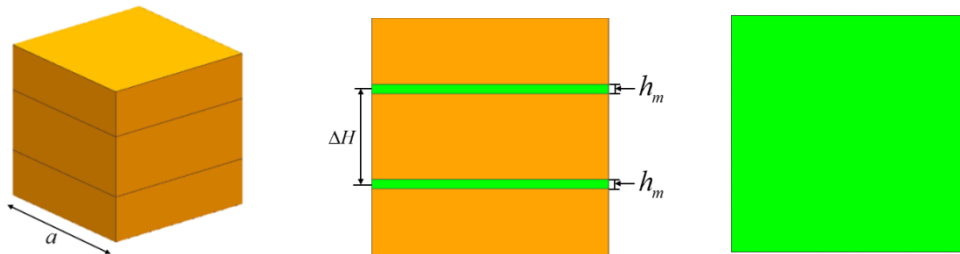


Figure 2. Unit cell with embedded double-layer membranes

Based on Eq.(3) and Eq.(4), after Floquet-Bloch boundary conditions are applied to the unit cell, dispersion characteristics of the unit cell are obtained. During the finite element analysis, in order to control the out-of-plane stiffness of the embedded membrane, we need adjust pre-stress applying to the membrane, so solid elements and membrane elements should be coupled to implement the simulation.

Analysis of dispersion characteristics

We take unit cells in Fig.1 and Fig.2 for examples to simulate dispersion curves of the unit cells with different h_m . Supposing that the pre-stress applied to the membrane along the z axis of Cartesian coordinate system $\{x, y, z\}$ is zero, the pre-stress along the x-axis is $T = 200 N/m$, the lattice constant is $a = 50 mm$, the distance between the double-layer membranes is $\Delta H = 30 mm$, the simulation results are shown in Fig.3(a)-(d) and Fig.4(a)-(d), where wave numbers are defined along the x-axis and the z-axis in the first Brillouin zone.

For the unit cell with a single-layer membrane in Fig.1, Fig.3(a)-(d) display dispersion curves while h_m are $0.01mm$, $0.09mm$, $0.25mm$ or $0.49mm$; similarly, corresponding to the unit cell with double-layer membranes with $\Delta H = 30mm$, Fig.4(a)-(d) display dispersion curves while h_m are $0.01mm$, $0.09mm$, $0.25mm$ or $0.49mm$. In all the figures, every red straight line is the tangent to a fitting curve to a series of data points among simulation results. According to the wave theory, the wave velocity c , the frequency f and the wave numbers \mathbf{k} satisfy

$$c = \frac{2\pi f}{|\mathbf{k}|} \quad (5)$$

Thus, the slope of every red straight line is corresponding to either the shear wave velocity or the longitudinal wave velocity.

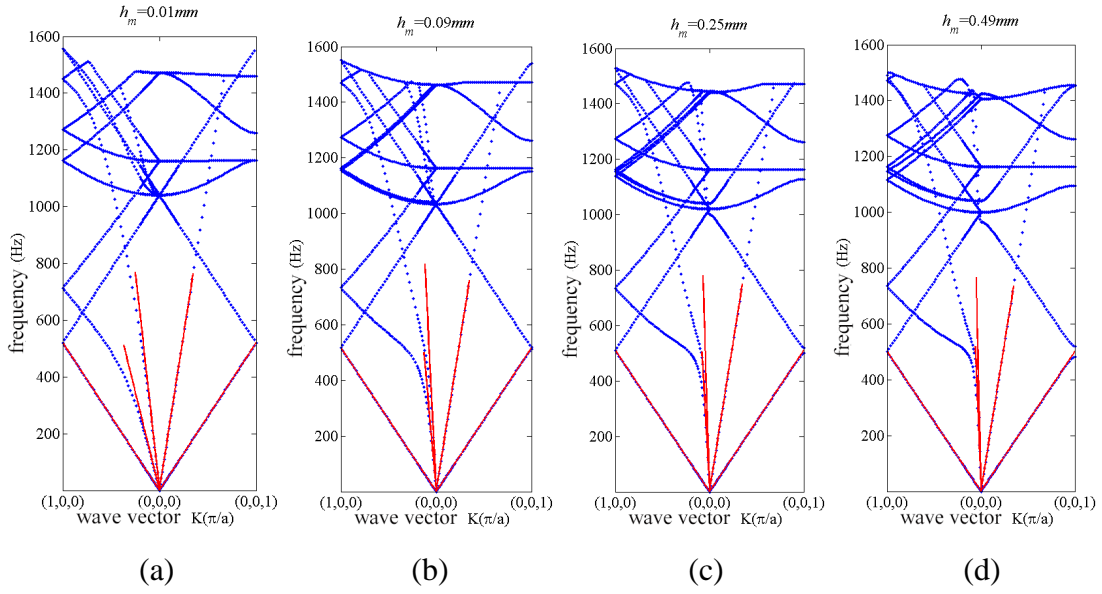


Figure 3. Dispersion curves of the unit cell with a single-layer membrane

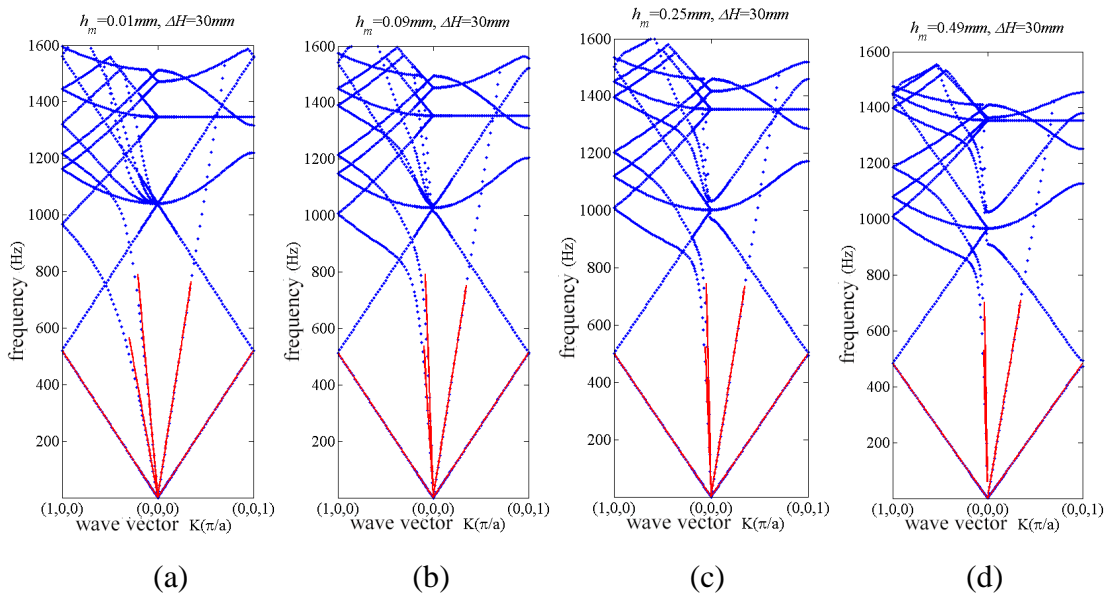


Figure 4. Dispersion curves of the unit cell with double-layer membranes

For an orthotropic material, the equivalent mass density ρ_0 can be calculated by

$$\rho_0 = \frac{\rho_m h_{mm} + \rho_r h_r}{h} \quad (6)$$

In a unit cell, ρ_m is the mass density of the membrane; h_{mm} is the total thickness of the membranes, for a unit cell with a single-layer membrane, $h_{mm} = h_m$, for a unit cell with double-layer membranes, $h_{mm} = 2h_m$; ρ_r is the mass density of rubber; h_r is the total thickness of rubber; h denotes the thickness of the unit cell and satisfies $h = h_r + h_{mm}$. In addition, equivalent modulus of elasticity of the unit cell E can be described as

$$E = \begin{bmatrix} E_{1111} & E_{1122} & E_{1133} & 0 & 0 & 0 \\ & E_{1111} & E_{1133} & 0 & 0 & 0 \\ & & E_{3333} & 0 & 0 & 0 \\ & \text{symmetry} & & E_{2323} & 0 & 0 \\ & & & & E_{1313} & 0 \\ & & & & & E_{1212} \end{bmatrix} \quad (7)$$

Where E is a symmetric matrix, E_{ijkl} stands for tensor of elasticity, and the subscripts $i, j, k, l = 1, 2, 3$ are corresponding to coordinate axes of x, y, z , respectively. Based on Christoffel's equation, we have

$$\left[\Gamma_{ij} - \rho_0 c^2 \delta_{ij} \right] \left[v_j \right] = 0 \quad (8)$$

in terms of

$$\Gamma = \left[\Gamma_{ij} \right] = \begin{bmatrix} E_{1111}n_1^2 + E_{1212}n_2^2 + E_{2323}n_3^2 & (E_{1122} + E_{1212})n_1n_2 & (E_{1133} + E_{2323})n_1n_3 \\ (E_{1122} + E_{1212})n_1n_2 & E_{1212}n_1^2 + E_{1111}n_2^2 + E_{2323}n_3^2 & (E_{1133} + E_{1212})n_2n_3 \\ (E_{1133} + E_{2323})n_1n_3 & (E_{1133} + E_{2323})n_2n_3 & E_{1212}n_1^2 + E_{1212}n_2^2 + E_{3333}n_3^2 \end{bmatrix} \quad (9)$$

and v_j , ($j = 1, 2, 3$) are displacement components of a point in the unit cell, n_1 , n_2 and n_3 represent direction cosines of wave numbers.

If λ_{\max} is the maximum eigenvalue of matrix Γ , velocities of longitudinal waves in directions (n_1, n_2, n_3) can be described by the formula

$$c_B = \sqrt{\frac{\lambda_{\max}}{\rho_0}} \quad (10)$$

For unit cells in Fig.1 and Fig.2, setting $a = 50\text{mm}$, $h_m = 0.5\text{mm}$, $\Delta H = 30\text{mm}$, we employ the asymptotic homogenization method (AHM) to calculate equivalent moduli of elasticity E_{ijkl} , ($i, j, k, l = 1, 2, 3$), and results are listed in Table 1. In addition, by further analyzing, we figure out average velocities of elastic waves propagating in the unit cells, including longitudinal wave velocities c_{Bx} and c_{Bz} , shear wave velocities c_{Gxy} , c_{Gxz} and c_{Gyz} , which are shown in Table 2. Meanwhile, we analyze dispersion characteristics of the unit cells and compute average velocities in the low frequency range according to dispersion curves (DCM). The results are also in Table 2. By comparison, it can be found that result errors between

AHM and DCM are very little, which verifies the simulation results.

Table 1. Equivalent moduli of elasticity of unit cells / MPa

Unit cell	E_{1111}	E_{2222}	E_{3333}	E_{2323}	E_{1313}	E_{1212}	E_{1122}	E_{1133}	E_{2233}
Single-layer membrane	2354.6	2354.6	46.9	2.7	2.7	810.4	733.9	41.6	41.6
Double-layer membranes	4662.3	4662.3	46.9	2.7	2.7	1618.0	1426.2	41.6	41.6

Table 2. Wave velocities calculated by both methods / m / s

Unit cell	Methods	c_{Bx}	c_{Bz}	c_{Gxz}	c_{Gxy}	c_{Gyz}
Single-layer membrane	AHM	1498.3	211.4	50.3	879.0	50.3
	DCM	1490.5	210.4	50.1	874.8	50.1
Double-layer membranes	AHM	2042.5	204.8	48.7	1203.2	48.7
	DCM	2024.6	202.9	48.4	1192.8	48.3

Influence of structure parameters of unit cells on wave velocities

In order to investigate acoustic characteristics of the 3-D membrane-embedded-type metamaterials, we can analyze equivalent elastic moduli of unit cells and ratios between the elastic moduli, or study propagation velocities of elastic waves in unit cells and ratios between the velocities. In this section, we will research the influence of structure parameters of unit cells on wave velocities and wave velocity ratios.

Influence of thickness of membranes on wave velocities

For a unit cell with a single-layer membrane, defining velocity ratios of T_I and T_{II} as $T_I = c_{Bx} / c_{Gxz}$, $T_{II} = c_{Bz} / c_{Bx}$, we calculate average velocities of an elastic wave in the unit cell and velocity ratios, where the unit cell has different h_m . The results are shown in Table 3 and Fig.5, where T_I describes the coupling relationship between longitudinal waves and shear waves; T_{II} indicates anisotropic characteristics of the unit cell.

Table 3. Average wave velocities in the unit cell with different h_m / m / s

h_m (mm)	$\sqrt{h_m}$ (\sqrt{mm})	c_{Bx}	c_{Bz}	c_{Gxz}	c_{Gxy}	c_{Gyz}
0.01	0.1	307.85	218.52	52.02831	138.43	51.98913
0.04	0.2	484.45	218.00	51.90377	261.15	51.86466
0.09	0.3	681.86	217.13	51.69815	385.87	51.65909
0.16	0.4	883.83	215.94	51.41430	509.66	51.37521
0.25	0.5	1085.10	214.44	51.05608	631.48	51.01708
0.36	0.6	1283.30	212.64	50.62853	750.64	50.58991
0.49	0.7	1476.90	210.57	50.13427	866.69	50.09949

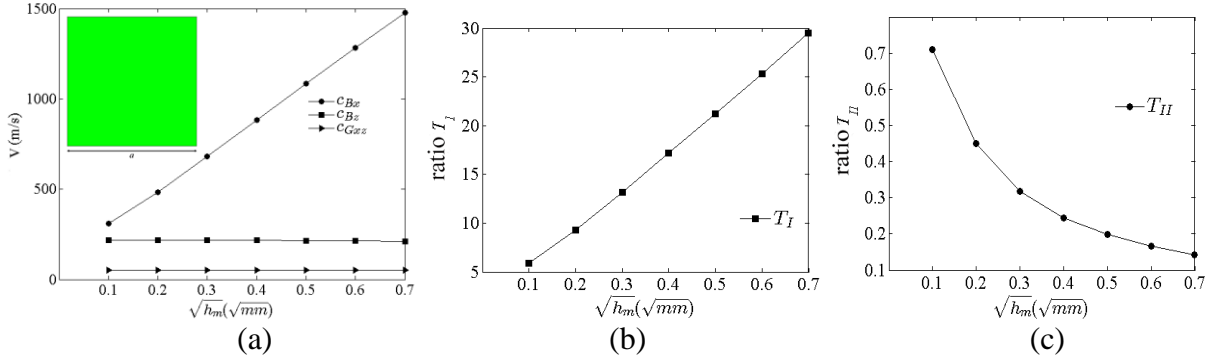
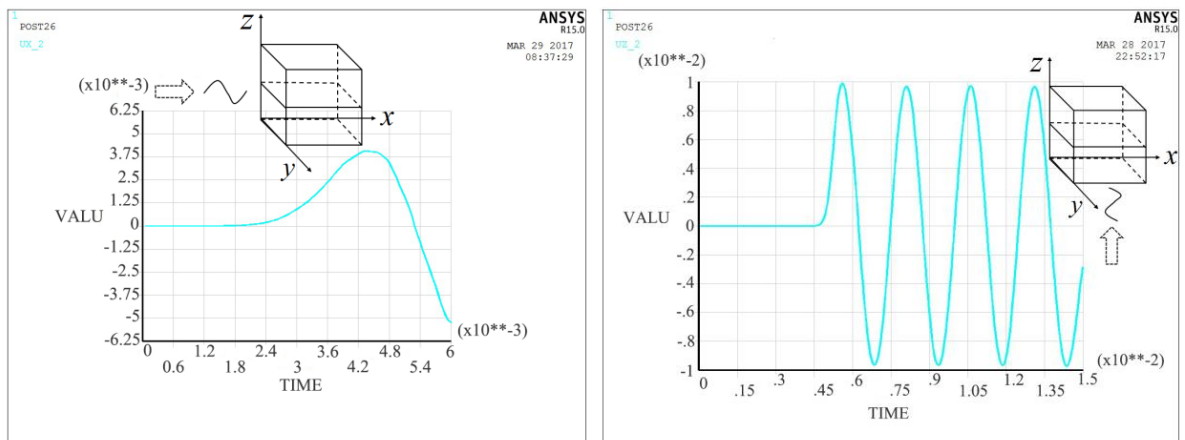


Figure 5. Relationship between wave velocities or wave velocity ratios and $\sqrt{h_m}$

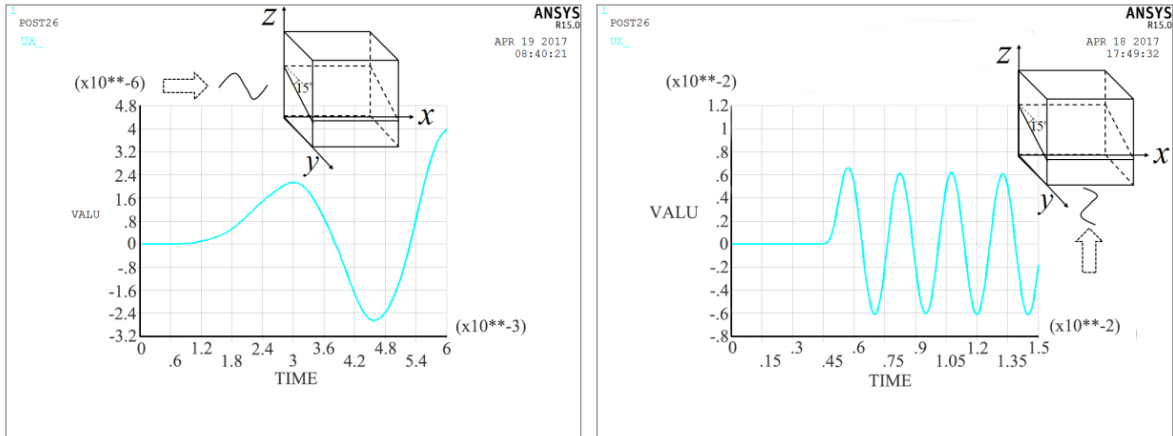
Seeing from Table 3 and Fig.5(a), we find that with the increase in $\sqrt{h_m}$, both the longitudinal wave velocity c_{B_x} and the shear wave velocity $c_{G_{xy}}$ increase greatly; however, the longitudinal wave velocity c_{B_z} and the shear wave velocities $c_{G_{xz}}$ and $c_{G_{yz}}$ change very little. Consequently, the velocity ratio of T_I increases linearly with $\sqrt{h_m}$, and the velocity ratio of T_{II} reduces significantly, as shown in Fig.5(b) and (c). Obviously, the thickness of membranes h_m has a great influence on the anisotropic characteristics of the unit cell.

Influence of inclination angles of membranes on wave velocities

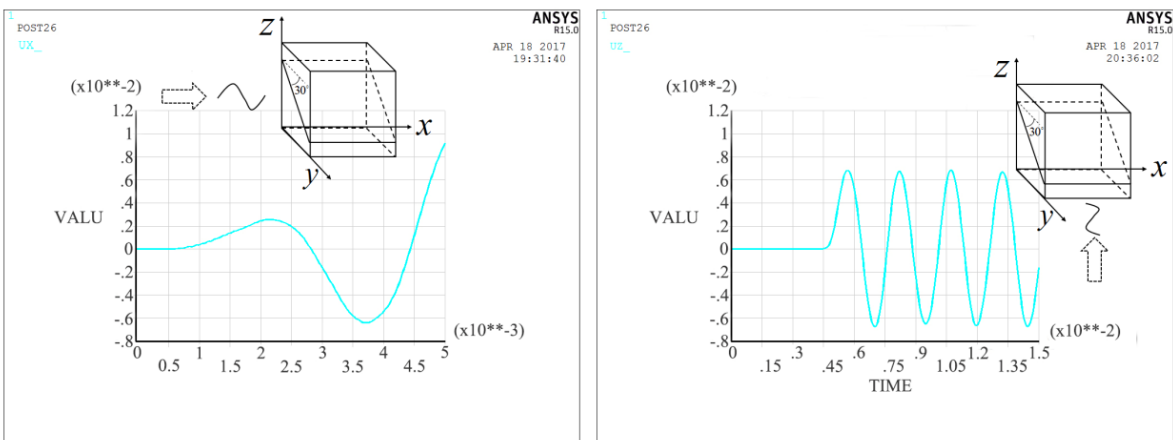
For a unit cell with a single-layer membrane, we set $h_m = 0.5\text{mm}$, $a = 50\text{mm}$ and use ψ to denote the inclination angle of the membrane, which is defined as the included angle between the normal vector of the membrane and the z axis. It is assumed that incident waves are either along the x-axis or the z-axis, we vary ψ from 0° to 45° with an interval of 15° , and employ the transient response full integration method (TRM) to simulate displacement-time curves. Simulation results are in Fig.6, where Fig.6(a)-(d) are corresponding to different ψ .



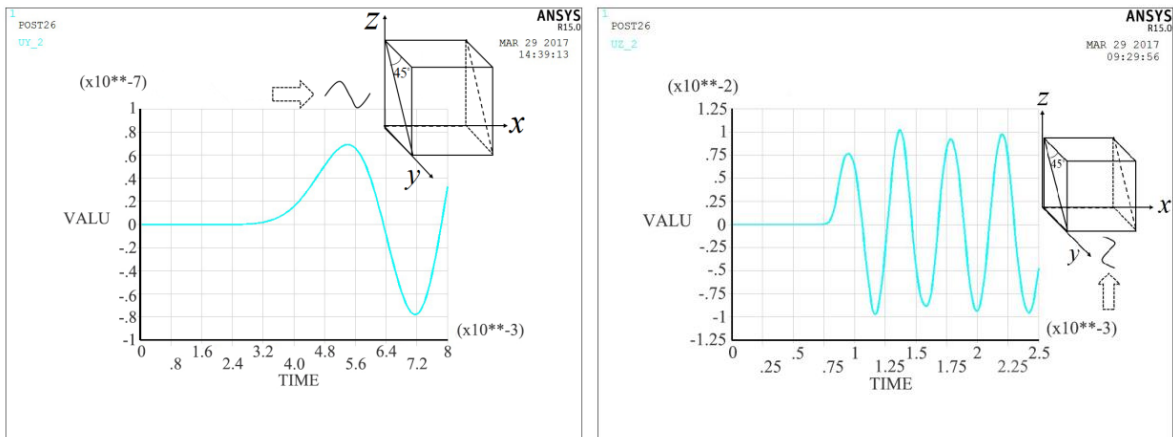
(a) $\psi = 0^\circ$



(b) $\psi = 15^\circ$



(c) $\psi = 30^\circ$



(d) $\psi = 45^\circ$

Figure 6. Displacement-time curves corresponding to different ψ

By further analysis, we calculate the average velocities of elastic waves, including the wave velocity along the x-axis v_x and the wave velocity along the z-axis v_z . Meanwhile, both the asymptotic homogenization method (AHM) and the dispersion characteristic analysis method (DCM) are also used to compute v_x and v_z . And all the wave velocities

calculated by the three methods are listed in Table 4. Seeing from Table 4, we find that wave velocities along the x-axis and the z-axis change smoothly while ψ increases from 0° to 30° , and when ψ reaches 45° , both v_x and v_z change greatly, especially the wave velocities along the z-axis.

Table 4. Average wave velocities in the unit cell with different ψ

ψ	0°		15°		30°		45°	
	v_x	v_z	v_x	v_z	v_x	v_z	v_x	v_z
AHM	1498	211	1443	210	1521	212	1840	1275
DCM	1491	210	1446	209	1518	204	1741	1232
TRM	1429	211	1418	211	1485	210	1768	1290

Influence of pre-stress applied to membranes on wave velocities

We take unit cells with a single-layer membrane or double-layer membranes for examples, and establish finite element models as shown in Fig.7.

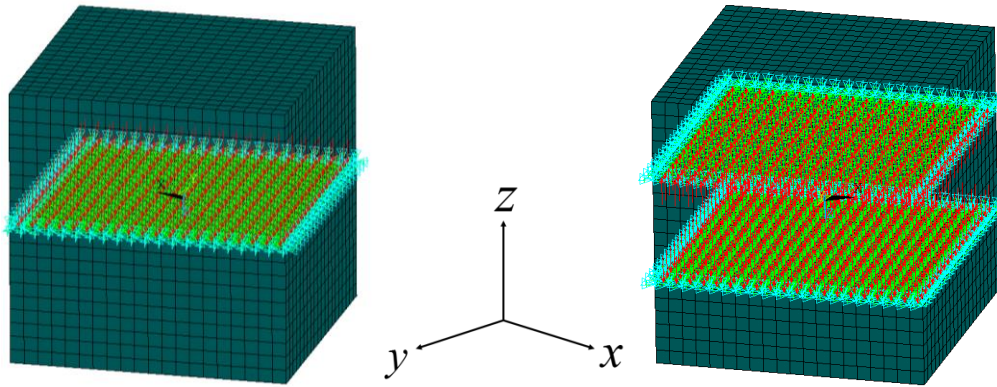


Figure 7. Finite element models of unit cells with pre-stressed membranes

It is assumed that $h_m = 0.5mm$, $a = 50mm$ and the in-plane pre-stress of the membranes is $T = 200N/m$. During the simulation process, a uniformly distributed load in the z axis is applied to the membranes to produce a certain pressure of P . In order to investigate the influence of the pressure on wave velocities, we vary the uniformly distributed load to make P applied to membranes change from $0MPa$ to $30MPa$. Here, ϕ is used to denote the velocity ratio, which is defined as $\phi = c_{Bz} / c_{Bz_0}$, where c_{Bz_0} and c_{Bz} stand for the average velocities of longitudinal waves while $P = 0MPa$ and $P \neq 0MPa$, respectively. Fig.8 shows the relationship curves between ϕ and P . In Fig.8(a), one curve is corresponding to the unit cell with a single-layer membrane, and the other corresponding to the unit cell with double-layer membranes. Fig.8(b) shows the simulation results of the unit cell with double-layer membranes, where ΔH is different. Seeing from Fig.8, we find that, for the unit cell with a single-layer membrane, the waves velocities along the z-axis c_{Bz} increases rapidly according to the increase in the pressure of P ; for the unit cell with double-layer membranes, c_{Bz} increases linearly with P . In addition, when P reaches $30MPa$, ϕ of the unit cell with a single-layer membrane becomes bigger than that of the unit cell with

double-layer membranes. And meanwhile, for the unit cell with double-layer membranes, the distance between double-layer membranes also has a great influence on wave velocities, and c_{Bz} changes with the increase in ΔH .

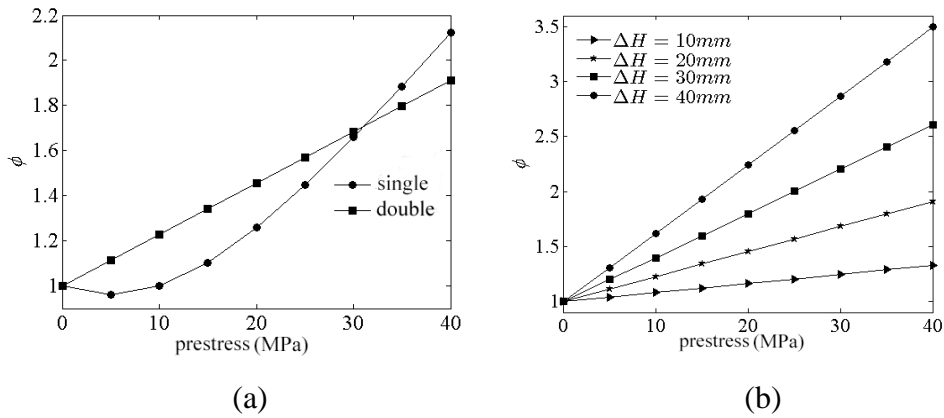


Figure 8. Relationship curves between ratios of the velocity and the pressure

Therefore, for a unit cell with an embedded single-layer membrane, we can adjust the pressure applied to the membrane to control the wave velocity along the z-axis; and for a unit cell with embedded double-layer membranes, we can change P and ΔH to make c_{Bz} reach a required value.

Acoustic characteristics of three-dimensional membrane-embedded-type metamaterials

In order to research acoustic characteristics of three-dimensional membrane-embedded-type metamaterials, we establish a finite element model as shown in Fig.9, which includes two parts, one is the isotropic rubber block and the other is the N -layer composite materials, where every layer of composite materials can be considered as a unit cell consisting of rubber and embedded single-layer or multi-layer membranes. Assuming that the incident wave is a plane wave with an incident angle of θ , the thickness of every unit cell is h , the equivalent modulus of elasticity of the unit cell in the i th layer is E_i ($i=1,2,\dots,N$), the thickness of a membrane is h_m , we simulate the wave propagation in the membrane-embedded-type metamaterial.

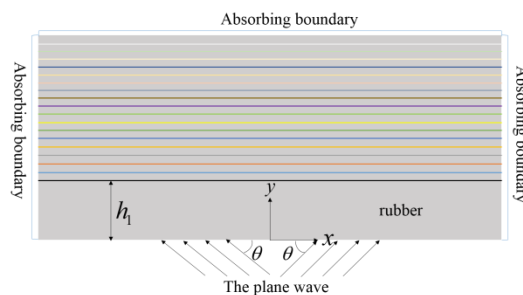


Figure 9. Finite element model

In this case, we set $E_1 = E_2 = \dots = E_N$, $h_m = 0.5mm$, the modulus of elasticity of rubber is $E_r = 7.8 \times 10^6 Pa$, the modulus of elasticity of membrane is $E_m = 2.1 \times 10^{11} Pa$, and simulation results are shown in Fig.10, where Fig.10(a) and (b) are corresponding to $\theta = 30^\circ$ and $\theta = 90^\circ$, respectively. Obviously, in the metamaterial, the wave propagation path bends at the interface between the rubber block and the composite materials, but in the N -layer composite

materials, the wave propagation direction does not change. That is because the equivalent modulus of elasticity of every unit cell is same.

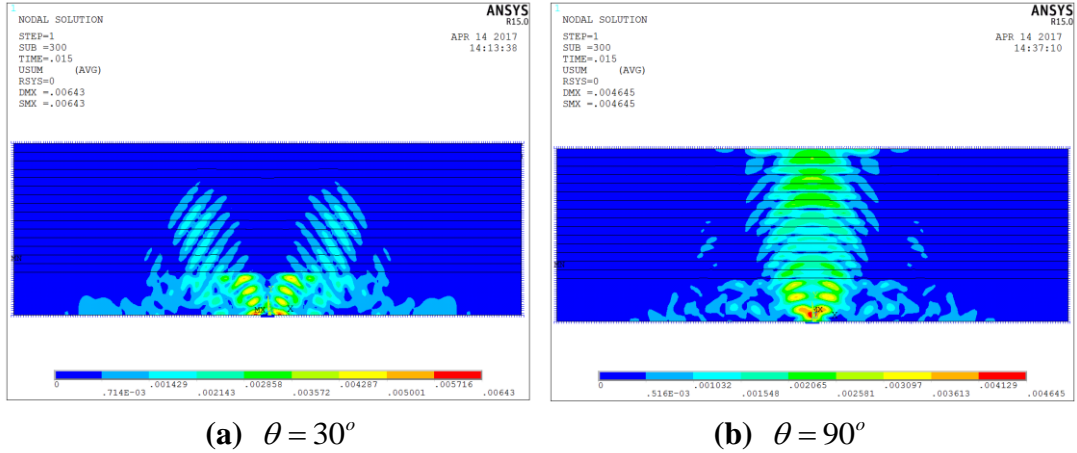


Figure 10. Color nephogram of the wave propagation

Next, in order to further research wave propagation in the membrane-embedded-type metamaterial, $E_i (i=1,2,\dots,N)$ are given in the form of a geometric progression with a scale factor q , and in this way, the equivalent modulus of elasticity of the unit cell in the i th layer can be expressed as

$$E_i(y) = E_0 q^{i-1} \quad (11)$$

Where, E_0 is a given value; $y = h_1 + h(i-1)$, and y represents the coordinate position of the unit cell in the i th layer, h_1 is the embedded depth of the first layer membrane.

In one case, we set $\theta = 30^\circ$, $E_0 = 7.8 \times 10^6 Pa$, $q = 10.0$; and in another case, we set $\theta = 30^\circ$, $E_0 = 2.1 \times 10^{11} Pa$, $q = 0.1$. Simulation results are shown in Fig.11, where Fig.11(a) and (b) are corresponding to $q = 10.0$ and $q = 0.1$, respectively. Clearly, it can be observed that the wave propagation path bends not only at the interface between the rubber block and the composite materials, but also at the interfaces between any two adjacent unit cells, and meanwhile, with the increase in E_i , the deflection angle of wave propagation becomes bigger and bigger.

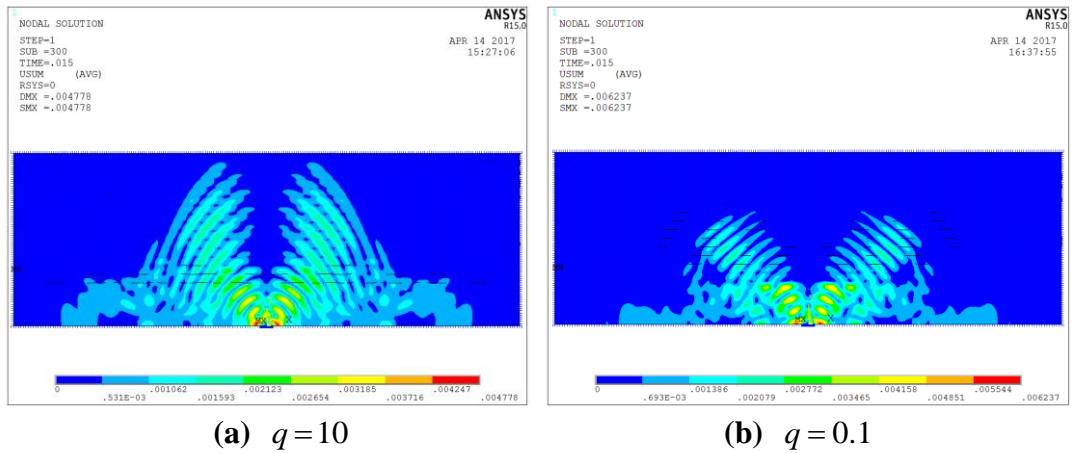


Figure 11. Color nephogram of the wave propagation

Conclusion

In this paper, we develop a new kind of 3-D membrane-embedded-type acoustic metamaterial, which is constructed by embedding high-modulus membranes into soft isotropic materials. Research shows the acoustic metamaterial has great potential for controlling propagation directions and propagation velocities of acoustic waves. The main conclusions are as follows:

Firstly, for unit cells of the acoustic metamaterial, the thickness of embedded membranes has a great influence on anisotropic characteristics of the unit cells. When the thickness of membranes varies in a certain range, the thicker the membrane is, the stronger the anisotropic characteristic of the unit cell is. Moreover, velocity ratios between longitudinal waves and shear waves almost increase linearly with the square root of the thickness of membranes.

Secondly, for unit cells of the acoustic metamaterial, inclination angles of embedded membranes have a certain influence on propagation velocities of elastic waves. When the inclination angle varies from 0° to 30° , wave velocities along the x-axis and the z-axis change smoothly; and when the inclination angle reaches 45° , the wave velocities change greatly, especially the wave velocities along the z-axis.

Thirdly, for unit cells of the acoustic metamaterial, the pre-stress applied to membranes has a great influence on wave velocities. When the pre-stress varies in a certain range, propagation velocities of longitudinal waves mostly increase linearly with the pre-stress. In addition, for unit cells with multi-layer membranes, the distance between adjacent membranes also has a great influence on wave velocities, and propagation velocities of longitudinal waves change significantly with the increase in the distance between adjacent membranes.

Finally, the propagation directions and propagation velocities of low frequency acoustic waves in the 3-D membrane-embedded-type acoustic metamaterial can be designed by simply analyzing and calculating the equivalent moduli of elasticity of unit cells. Furthermore, the control of acoustic waves can be realized by adjusting structure parameters of every unit cell, including the thickness of membranes, the inclination angles of membranes and the pre-stress applied to membranes.

Acknowledgement

This research was financially supported by the National Science Foundation No.11372059 and No.11272073

References

- [1] Andrew N. Norris, Acoustic metafluids, *J. Acoust. Soc. Am.*, Vol.125, No. 2, p: 839-849, 2009
- [2] Rui-Qi Li, Xue-Feng Zhu, Bin Liang, Yong Li, Xin-Ye Zou, Jian-Chun Cheng, A broadband acoustic omnidirectional absorber comprising positive-index materials, *Appl. Phys. Lett.*, Vol. 99, p:193507 (1-3), 2011
- [3] Mohamed Farhat, Sebastien Guenneau, and Stefan Enoch, Broadband cloaking of bending waves via homogenization of multiply perforated radially symmetric and isotropic thin elastic plates, *Physical Review B* 85, 020301(R) (2012)
- [4] Yang Z, Mei J, Yang M, et al. Membrane-type acoustic metamaterials with negative dynamic mass[J]. *Physical Review Letters*, 2008, 101(20): 204301
- [5] Jun Mei, Guancong Ma, Min Yang, Zhiyu Yang, Weijia Wen, Ping Sheng, Dark acoustic metamaterials as super absorbers for low-frequency sound
- [6] Fuyin Ma, Jiu Hui Wu, Meng Huang, Wei-quan Zhang and Si-wen Zhang. A purely flexible lightweight membrane-type acoustic metamaterial[J]. *Journal of Applied Physics*, 2015, 48: 175105
- [7] F. Langfeldt, J. Riecken, W. Gleine, O. von Estorff. A membrane-type acoustic metamaterial with adjustable acoustic properties[J]. *Journal of Sound and Vibration*, 2016, 373: 1-18
- [8] Bogdan-Ioan Popa, Lucian Zigoneanu, and Steven A. Cummer, Tunable active acoustic metamaterials, *Physical Review B*, 88(2013), 024303